

Supporting Information

Carboxylesterase-activated near-infrared fluorescence probe for highly sensitive imaging liver tumor

Renfeng Jiang,^{‡, c} Yuqing Xia,^{‡, b} Qian Liu,^b Hongshuai Zhang,^{a, b*} Xuefeng Yang,^{a, b}

Longwei He,^{c,*} Dan Cheng^{a, b, c*}

^a *Department of Gastroenterology, the Affiliated Nanhua Hospital, Hengyang Medical School, University of South China, Hengyang 421002, Hunan Province, China*

^b *Hunan Provincial Clinical Research Center for Metabolic Associated Fatty Liver Disease, Clinical Research Institute, the Affiliated Nanhua Hospital, Hengyang Medical School, University of South China, Hengyang 421002, Hunan, China* ^c *Hunan Province Cooperative Innovation Center for Molecular Target New Drug Study, School of Pharmaceutical Science, Hengyang Medical School, University of South China, Hengyang 421002, Hunan, China*

*Corresponding Author.

E-mail: hongshuai_zhang@hnu.edu.cn, helongwei0110@163.com, flychand0110@163.com

Supporting Information

Table of content

1.	Materials and General Experimental Methods	S3
2.	Spectrometric Studies	S3
3.	Calculation of Fluorescence Quantum Yield	S3
4.	Calculation of Reaction Rate Constants of NCES and CES	S3
5.	Fluorescence Microscopic Studies	S3-S4
6.	<i>In vivo</i> Imaging Studies	S4-S5
7.	Biodistribution studies	S5
8.	Histology and Immunohistochemical staining	S5
9.	Visualization of CES in clinical serum	S5
10.	Supplemental Figures	S5-S14
11.	References	S15

1. Materials and General Experimental Methods

Unless otherwise stated, all reagents were purchased from commercial suppliers and used without further purification. Solvents used were purified by standard methods prior to use. Twice-distilled water was used throughout all experiments. NMR spectra were recorded on a Bruker-500 spectrometer, using TMS as an internal standard. Photoluminescent spectra were recorded at room temperature with a HITACHI F7100 fluorescence spectrophotometer (1 cm standard quartz cell). The pH measurements were carried out on a Mettler-Toledo Delta 320 pH meter; the fluorescence images were acquired with a confocal laser scanning microscope (Nikon); The *in vivo* (living mice) imaging was carried out using the FUSION FX imaging system (Vilber Lourmat); TLC analysis was performed on silica gel plates and column chromatography was conducted over silica gel (mesh 200-300).

2. Spectrometric Studies

Measurement of photophysical properties. For photophysical characterization, probe NCES was dissolved in DMSO to make the stock solutions (500 μM), which were diluted to 5 μM as the testing solutions with 25 mM PBS (pH 7.4). Absorption and fluorescence spectroscopic studies were performed on a UV2600 spectrophotometer and a Hitachi F-7100 fluorescence spectrophotometer.

3. Calculation of Fluorescence Quantum Yield

Fluorescence quantum yield was determined using optically matching solutions of ICG ($\Phi_f = 0.13$ in DMSO)¹ as the standard and the quantum yield was calculated using the following equation:

$$\Phi_s = \Phi_r(A_r F_s / A_s F_r) (n_s^2 / n_r^2)^2$$

where, s and r denote sample and reference, respectively. A is the absorbance. F is the relative integrated fluorescence intensity and n is the refractive index of the solvent.

4. Calculation of Reaction Rate Constants of NCES and CES

The reaction of NCES probe (5 μM) with CES (2 U/mL) in PBS/DMSO (v/v = 9/1, 25 mM, pH 7.4) buffer solution at 37 °C was monitored using the fluorescence intensity at 776 nm ($\lambda_{\text{ex}} = 680$ nm). The fluorescence intensities were recorded by the addition of CES (2 U/mL) to the mixture containing NCES probe (5 μM) and this reaction system presents an excess of CES. Therefore, the following fluorescence intensities fitted to the pseudo-first order equation was available to determine the reaction rate constant:

$$\text{Ln} ((F_{\text{max}} - F_t) / F_{\text{max}}) = -k't^3$$

Where F_t and F_{max} are the fluorescence intensities at 776 nm at times t and the maximum value obtained after the reaction was complete. k' is the apparent rate constant. The negative slope of the line provides the apparent rate constant: $k' = 0.06463 \text{ min}^{-1}$.

5. Fluorescence Microscopic Studies

Cell culture. HepG2, A549 and HeLa cells were cultured in high glucose Dulbecco's Modified Eagle Medium (DMEM, Hyclone) supplemented with 10% fetal bovine serum (FBS, BI), and 1% antibiotics (100 U/mL penicillin and 100 $\mu\text{g}/\text{mL}$ streptomycin, Hyclone) at 37 °C and 5% CO_2 . Cells were carefully harvested and split when they reached 80% confluence to maintain exponential growth.

Fluorescence microscopic imaging. All the experiments were conducted in live cells. Microscopic imaging uses Nikon confocal microscope. $\lambda_{\text{ex}}=640$ nm, $\lambda_{\text{em}}=662-737$ nm.

For CES content in diverse cell lines imaging experiments, HepG2, A549 and HeLa cells were incubated with 5 μM NCES for 30 min. Cell imaging was performed after washing the cells with PBS for three times.

For CES inhibition imaging experiments, HepG2 cells were incubated with ABESF (0, 0.1, 0.5, 1 mM) for 0.5 h, respectively, and then the cells were incubated with 5 μM NCES probe for 0.5 h. Cell imaging was performed after washing the cells with PBS for three times. For drug screening imaging experiments, HepG2 cells were incubated with donepezil, carbaryl and enalapril at concentrations of 0.2 mM for 1 h, respectively, and then the cells were incubated with 5 μM NCES probe for 0.5 h. Cell imaging was performed after washing the cells with PBS for three times.

For stimulation imaging experiments, HepG2 cells were pre-treated with LPS (3, 5 $\mu\text{g}/\text{mL}$) for 12 h or 1 mM H_2O_2 for 1 h or 3.5 h. Then, these cells were incubated with 5 μM NCES for 30 min. Cell imaging was performed after washing the cells with PBS for three times.

Cell cytotoxicity in MTT assay. Cells were plated in 96-well flat-bottomed plates at 1×10^5 cells per well and allowed to grow overnight prior to exposure to NCES. Then the MTT (0.5 mg/mL) reagent was added for 4 h at 37 °C and DMSO (100 $\mu\text{L}/\text{well}$) was further incubated with cells to dissolve the precipitated formazan violet crystals at 37 °C for 15 min. The absorbance was measured at 490 nm by a multidetection microplate reader. The following formula was used to calculate the viability of cell growth: Cell viability = (mean of *A* value of treatment group / mean of *A* value of control).

Co-localization Imaging Experiment. HepG2 cells were incubated with 5 μM NCES for 30 min and then co-staining with Mito-Tracker Green or Lyso-Tracker Green for 15 min, respectively. These cells were all washed by PBS buffer for three times before imaging. $\lambda_{\text{ex}}=488$ nm, $\lambda_{\text{em}}=500-550$ nm.

Flow Cytometry Analysis. Flow cytometry was employed to determine inhibition effect and drug screening of CES with probe NCES. HepG2 cells in 6-well plate were precultured for 24 h and pretreated with AEBSF (0, 0.1, 0.5, 1 mM) for 0.5 h or donepezil, carbaryl and enalapril at concentrations of 0.2 mM for 1 h, respectively, and then the cells were incubated with 5 μM probe NCES for 30 min. After incubation, the cells were treated with trypsin, washed twice with medium and subjected to flow cytometry analysis. $\lambda_{\text{ex}}=640$ nm.

6. *In vivo* Imaging Studies

All animal experiments were performed in accordance with the Experimental Animal Ethics Committee of the University of South China. All BALB/c mice (18-20 g) were obtained from Hunan SJA Laboratory Animal Co. Ltd. and operated in accordance with University of South China guidelines on the care and use of animals for scientific purposes.

Imaging of CES *in vivo*. The experiment can be divided into two groups. For the control group, mice were preinjected with PBS (100 μL) for real-time recording of 2 h. For the experimental group, mice were preinjected with NCES (100 μL , 200 μM) probe for real-time recording of 2 h. Then, they were used for biodistribution studies, respectively.

Visualization of CES in tumor-bearing mice. For establishing a mouse tumor model, the HepG2 cells (5×10^7 cells) were chose to transplant under the flank of approximately 18-20 g female BALB/c mice for 20 days. For imaging of tumor, the mice were treated with NCES probe (20 μL ,

100 μM) by spraying way for *in vivo* imaging. All the mice were anaesthetized and performed *in vivo* imaging under a FUSION FX imaging system. $\lambda_{\text{ex}} = 680 \text{ nm}$, $\lambda_{\text{em}} = 735\text{-}765 \text{ nm}$.

7. Biodistribution studies

All studies were completed in 18-20 g BALB/c mice. For biodistribution studies, after administration of NCES, mice were killed at the indicated timepoints and their organs (heart, liver, spleen, lung, kidney) for fluorescence measurements. The imaging was carried out using a FUSION FX imaging system. $\lambda_{\text{ex}} = 680 \text{ nm}$, $\lambda_{\text{em}} = 735\text{-}765 \text{ nm}$.

8. Histology and Immunohistochemical staining

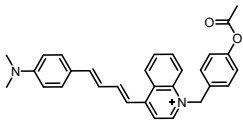
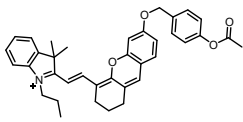
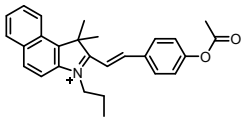
All tissues of Kunming mice were fixed in 10% formaldehyde immediately after sacrifice. Histological examination was according to a conventional method, and stained with hematoxylin and eosin (H&E). Classify and record the morphology of any observed lesions was according to classification criteria.⁴

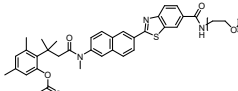
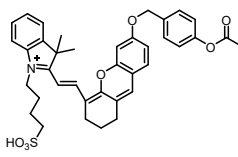
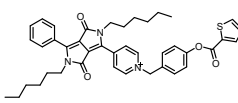
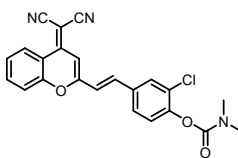
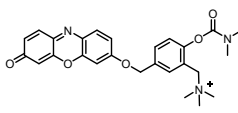
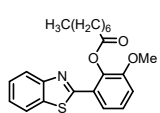
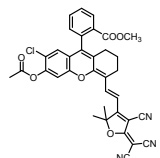
9. Visualization of CES in clinical serum

All experiments with human samples were approved by the medical ethics committee of The First Affiliated Hospital (University of South China). Informed consent was obtained from all participants. Normal serum and clinical diabetes serum were incubated with NCES (5 μM , 30 min). All the sample were performed *in vitro* imaging under a FUSION FX imaging system. $\lambda_{\text{ex}} = 680 \text{ nm}$, $\lambda_{\text{em}} = 735\text{-}765 \text{ nm}$.

10. Supplemental Figures

Table S1. Summary of representative reported CES fluorescent probes.

Structure	λ_{ex} (nm)	λ_{em} (nm)	LOD	K_m	Biological application	Reference
	443 nm	593 nm	$3.04 \times 10^{-6} \text{ U/mL}$	25.19 μM	Imaging tumor <i>in vivo</i>	5
	670 nm	705 nm	$4.5 \times 10^{-3} \text{ U/mL}$	----	Imaging of CES in Zebra-fish	6
	520 nm	575 nm	$1.2 \times 10^{-4} \text{ U/mL}$	18 mM	Imaging of CES in tissues and serum	7

	332 nm	455 nm	0.5 nM	4.33 ±0.22 mM	Imaging of CES in live tissues	8
	670 nm	706 nm	3.4×10^{-3} U/mL	----	Imaging of CES in living cells	9
	465 nm	542 nm	1.6×10^{-5} U/mL	----	Imaging of CES in liver tissues	10
	540 nm	685 nm	0.013 U/mL	0.21 μM	Imaging of CES in the orthotopic liver tumor	11
	550 nm	582 nm	0.017 U/mL	29.57 mM	Imaging of CES in living cells, mice brains and tissues	12
		489 nm	hCES1b/hCES1c		Imaging of CES in Zebra-fish	13
	304 nm	nm/374 nm	0.128 μg/mL /	----		
	680 nm	776 nm	5.24 mU/mL	15.244 μM	Imaging of CES in living cells, <i>in vivo</i> and clinical serum	This work

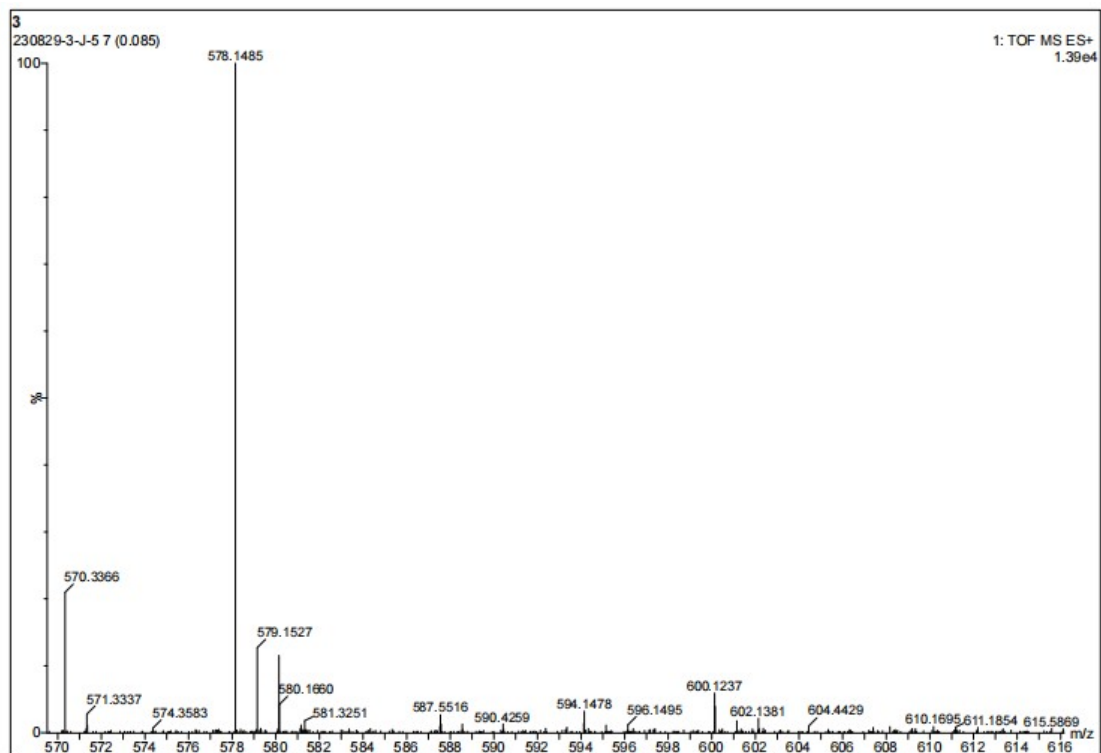


Fig.S1. The ESI mass spectrum of compound NCES in the presence of CES.

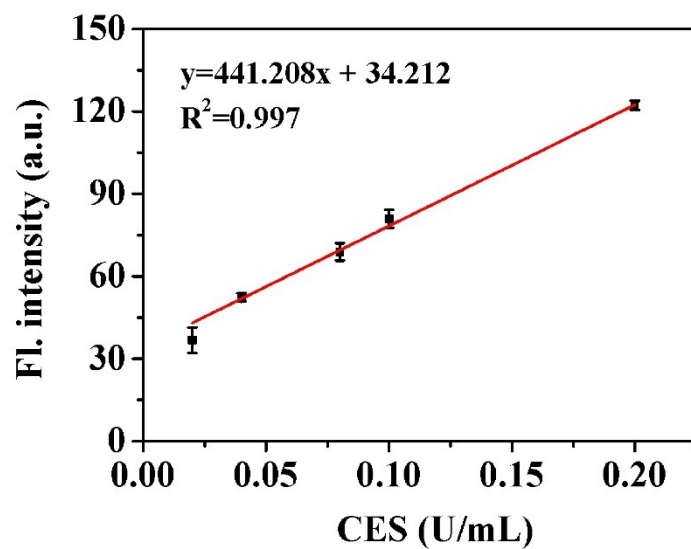


Fig. S2. Linear correlation between $F_{776\text{nm}}$ and CES concentrations in PBS/DMSO (v/v = 9/1, 25 mM, pH 7.4) buffer solution.

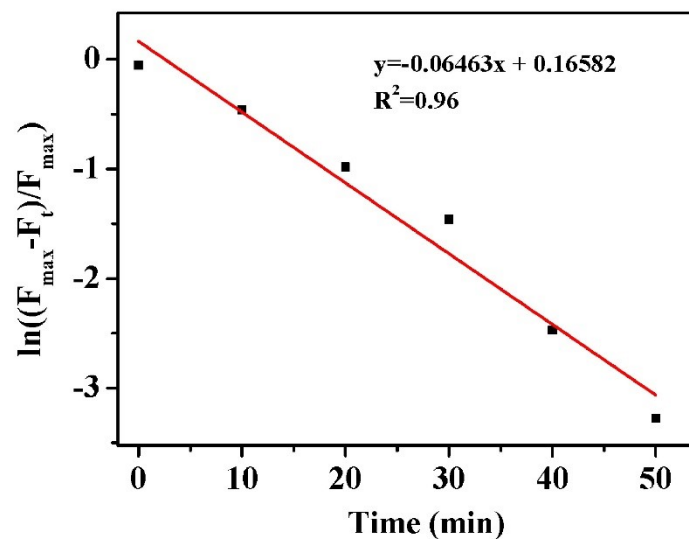


Fig. S3. Pseudo first-order kinetic plot of reaction of NCES (5 μM) with CES (2 U/mL) in PBS/DMSO (v/v = 9/1, 25 mM, pH 7.4) buffer solution. slope = $-0.06463 \text{ min}^{-1}$.

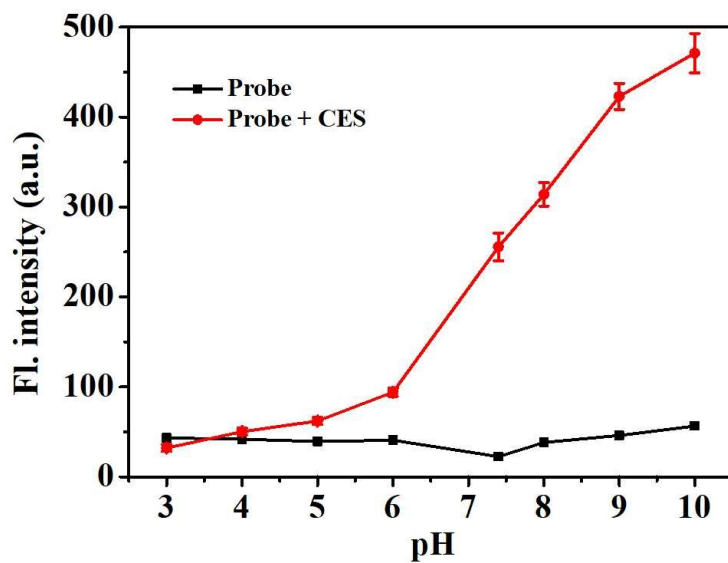


Fig. S4. Effects of pH on the fluorescence of probe NCES (5 μM) reacting with CES (0.05 U/mL). $\lambda_{\text{ex}}/\lambda_{\text{em}} = 680/776 \text{ nm}$.

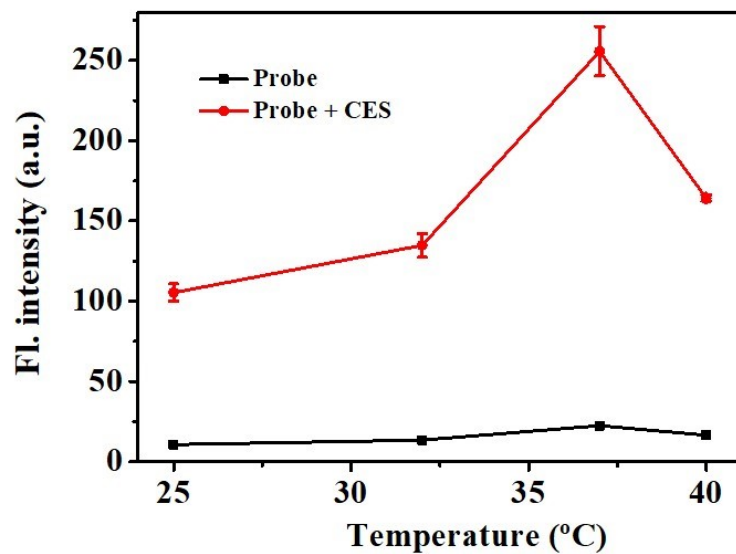


Fig. S5. Effects of temperature on the fluorescence of probe NCES (5 μM) reacting with CES (2.00 U/mL). $\lambda_{\text{ex}}/\lambda_{\text{em}}$ = 680/776 nm.

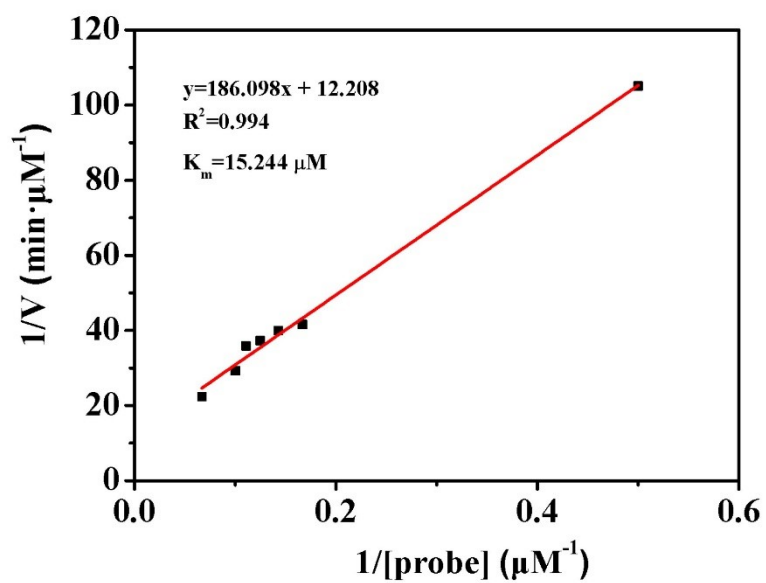


Fig. S6. Lineweaver–Burk plot for the enzymatic reaction. The NCES (2-15 μM) were incubated with CES (2.00 U/mL) in PBS/DMSO (v/v = 9/1, 25 mM, pH 7.4) buffer solution at 37 $^{\circ}\text{C}$ for 10 min. $\lambda_{\text{ex}}/\lambda_{\text{em}}$ = 680/776 nm.

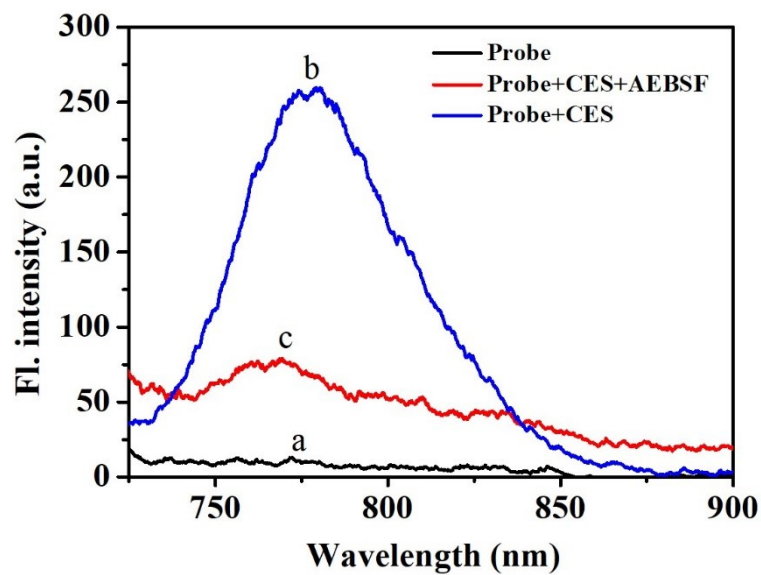


Fig. S7. Fluorescence emission spectra of different reaction systems. (a): NCES probe (5 μM) in PBS/DMSO (v/v = 9/1, 25 mM, pH 7.4) buffer solution; (b): (a) + CES (2 U/mL); (c): (b) + AEBSF (500 μM). All the reactions were performed at 37 $^{\circ}\text{C}$. $\lambda_{\text{ex}} = 680$ nm.

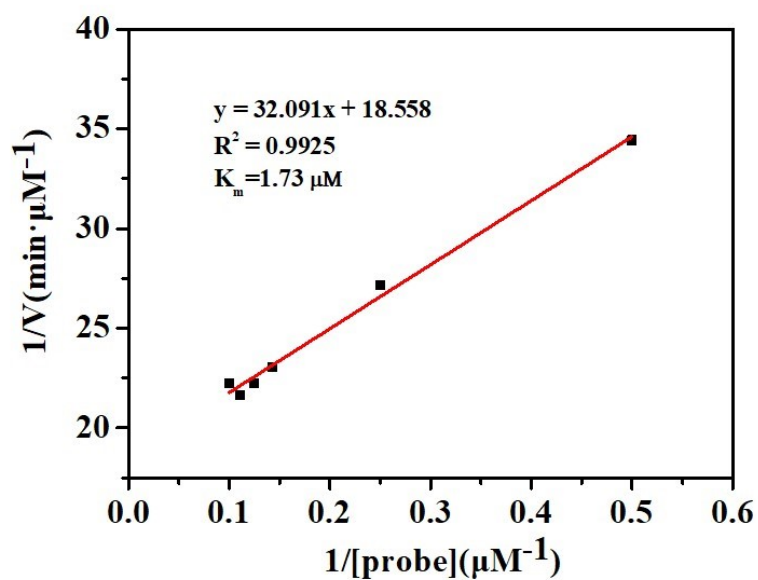


Fig. S8. Michaelis-Menten enzyme kinetics in the presence of AEBSF inhibitor. The NCES (2-15 μM) and CES (2.00 U/mL) were incubated with AEBSF (500 μM) in PBS/DMSO (v/v = 9/1, 25 mM, pH 7.4) buffer solution at 37 $^{\circ}\text{C}$ for 10 min. $\lambda_{\text{ex}}/\lambda_{\text{em}} = 680/776$ nm.

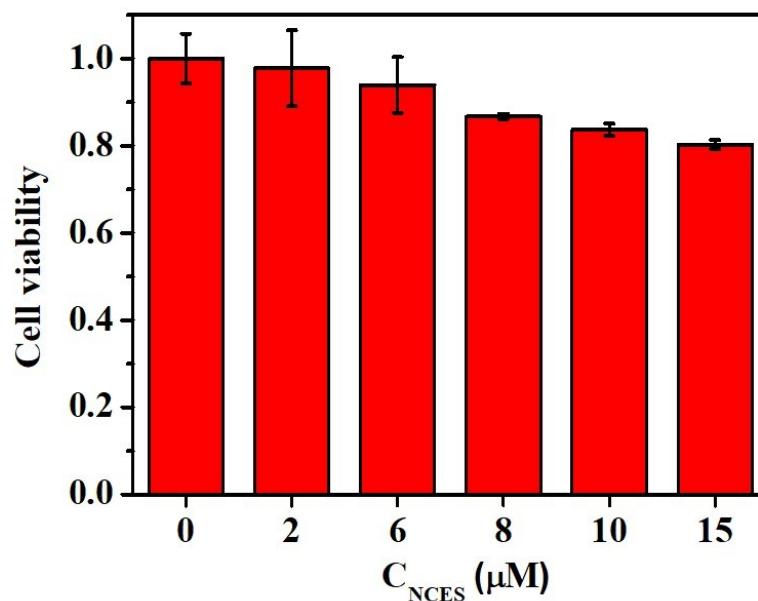


Fig. S9. Cytotoxicity of NCES for HepG2 cells. Cells were incubated with the probe at corresponding concentrations for 24 h.

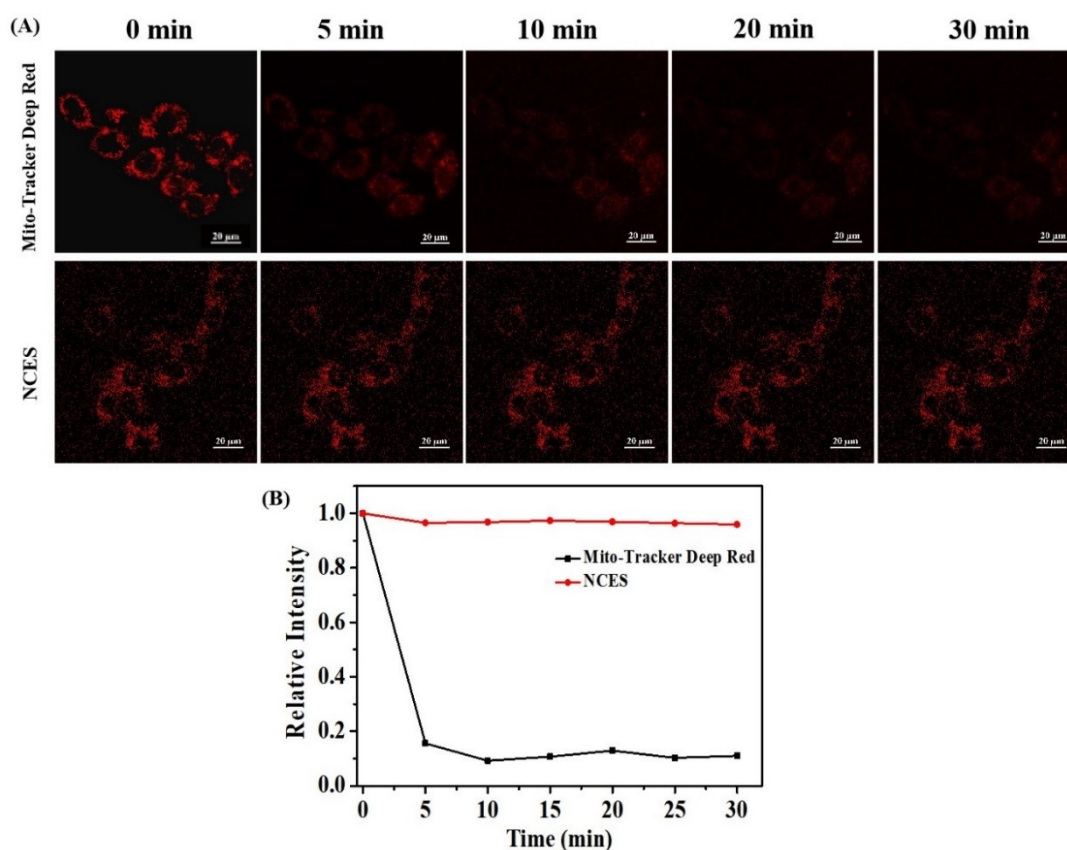


Fig. S10. (A) Confocal fluorescence images of living HepG2 cells cultured with NCES probe and Mito-Tracker Deep Red with continuous irradiation using confocal microscope with the same parameters. (B) Relative fluorescence intensity of cells from the images of NCES and Mito-Tracker Deep Red. Scale bar = 20 μm. For NCES and Mito-Tracker Deep Red: λ_{ex} = 640 nm and λ_{em} = 662–737 nm.

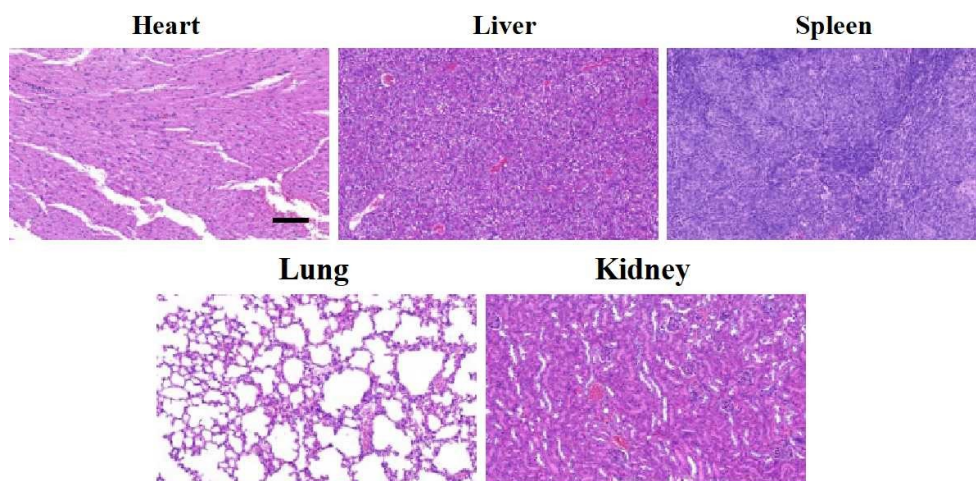


Fig. S11. Representative histological sections (H&E staining) for main organs of the mice one day after intravenous injection of NCES (200 μ M, 100 μ L). Scale bar = 100 μ m.

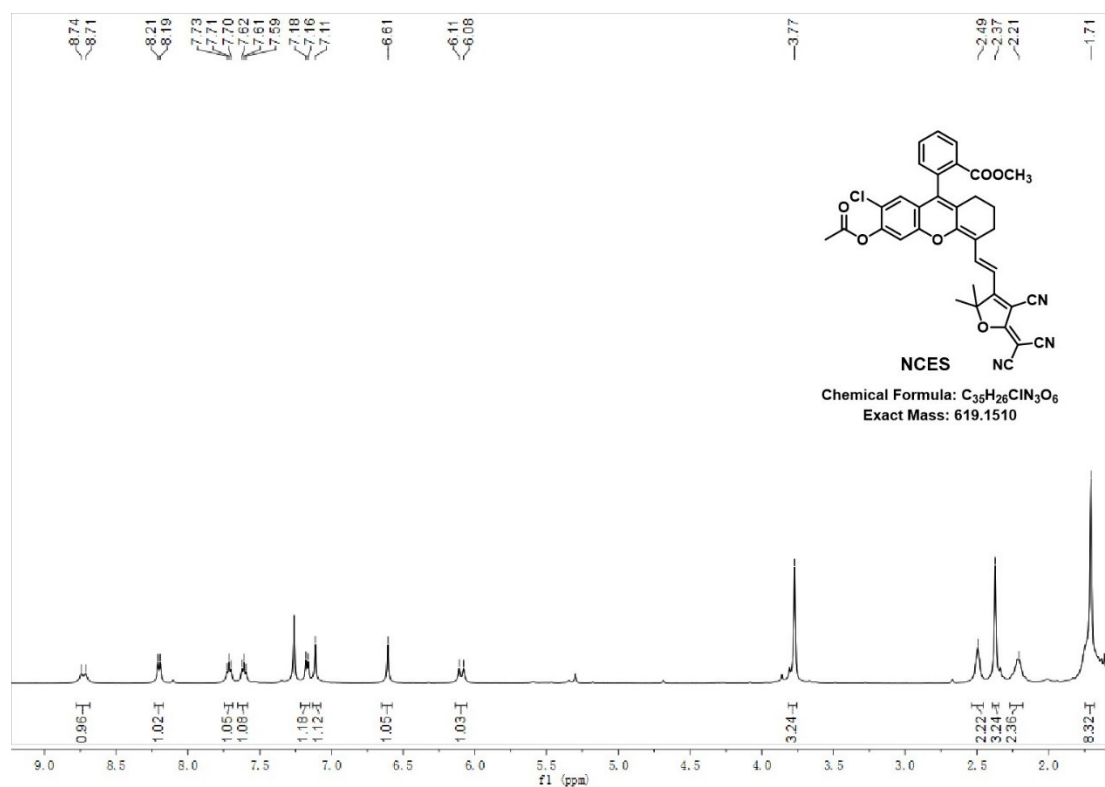


Fig. S12. The ^1H NMR spectrum of compound NCES (CDCl_3).

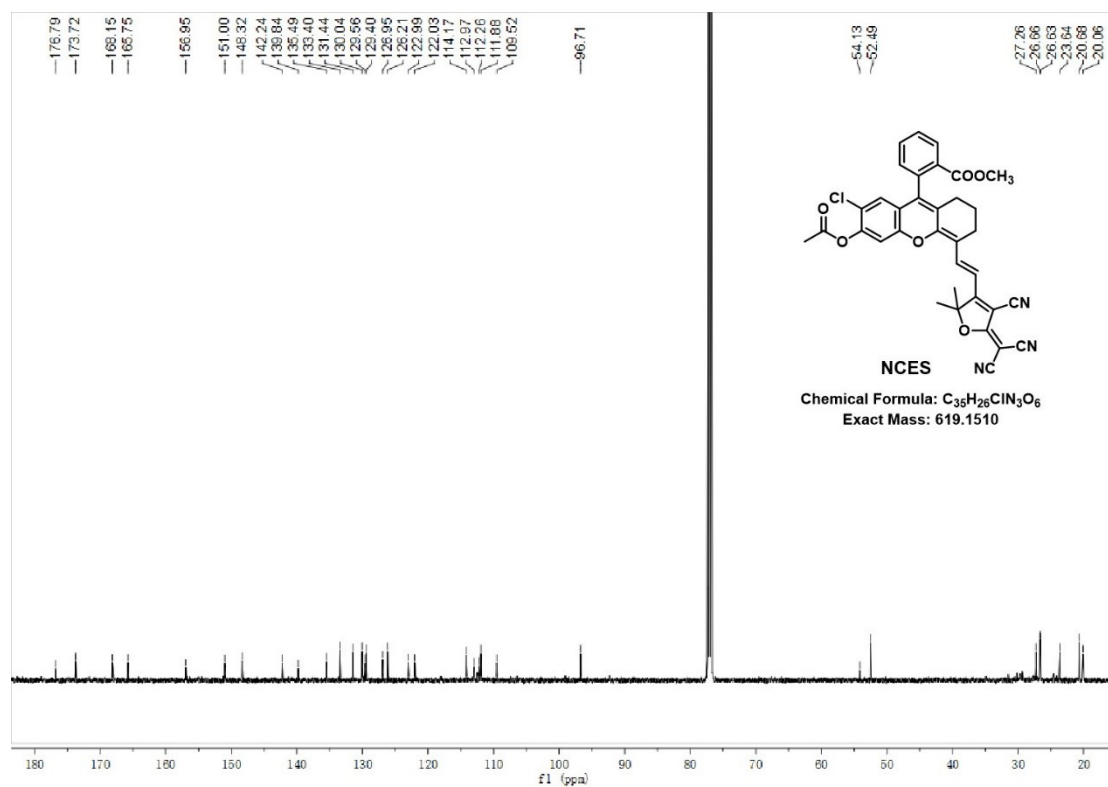


Fig. S13. The ^{13}C NMR spectrum of compound NCES ($CDCl_3$).

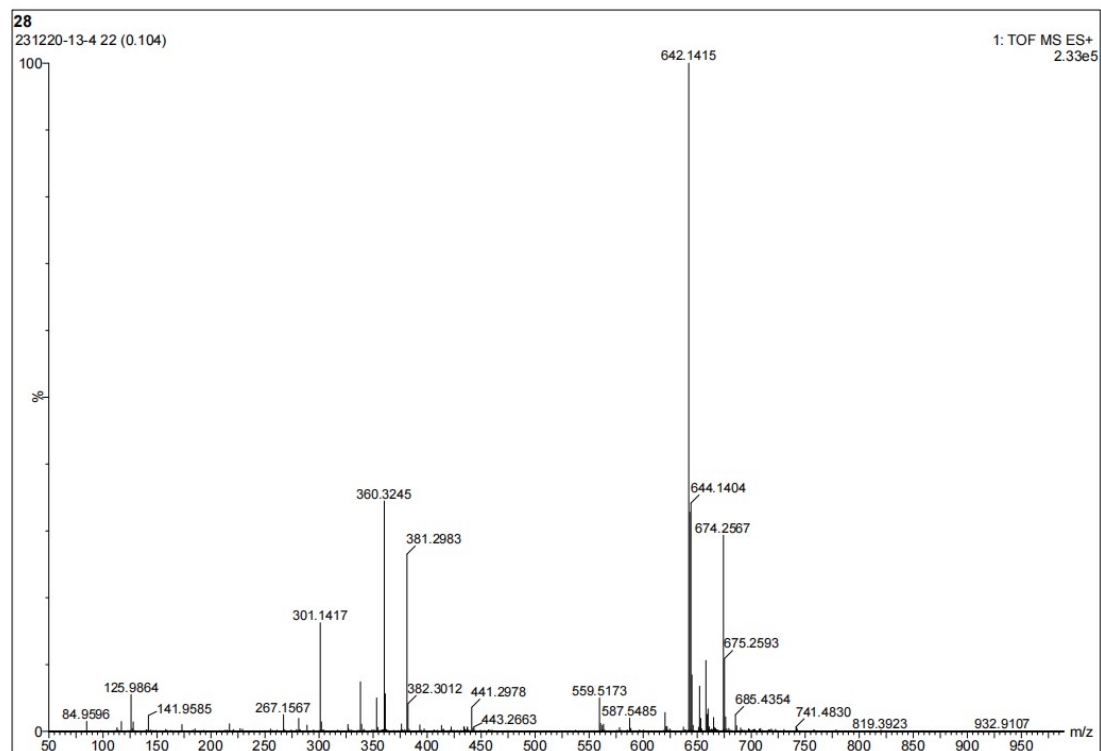


Fig. S14. The ESI mass spectrum of compound NCES.

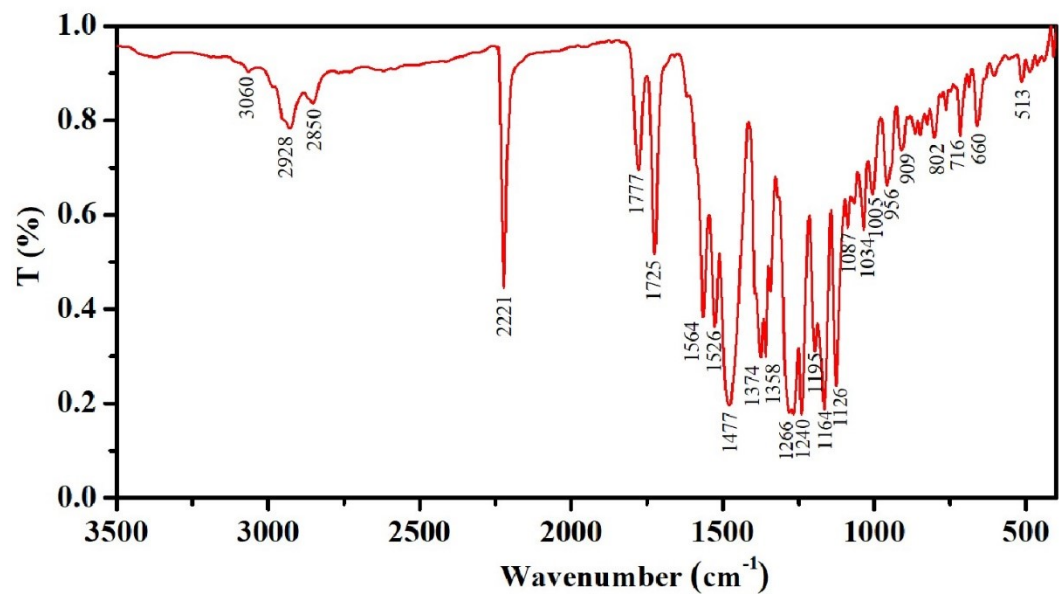


Fig.S15. The FTIR spectrum of compound NCES.

11. References

- [1] K. Rurack and M. Spieles, *Anal. Chem.*, 2011, **83**, 1232.
- [2] Z. Qin, T. B. Ren, H. Zhou, X. Zhang, L. He, Z. Li, X. B. Zhang and L. Yuan, *Angew. Chem. Int. Ed.*, 2022, **61**, e202201541.
- [3] T. J. Dale and J. Rebek, *J. Am. Chem. Soc.*, 2006, **128**, 4500–4501.
- [4] F. Yu, P. Li, G. Li, G. Zhao, T. Chu and K. Han, *J. Am. Chem. Soc.*, 2011, **133**, 11030–11033.
- [5] Y. L. Qi, H. R. Wang, L. L. Chen, B. Yang, Y. S. Yang, Z. X. He and H. L. Zhu, *Anal. Chem.*, 2022, **94**, 4594–4601.
- [6] D. Li, Z. Li, W. Chen and X. Yang, *J Agric Food Chem.*, 2017, **65**, 4209–4215.
- [7] H. Zhou, J. Tang, J. Zhang, B. Chen, J. Kan, W. Zhang, J. Zhou and H. Ma, *J. Mater. Chem. B.*, 2019, **7**, 2989–2996.
- [8] S. J. Park, H. W. Lee, H. R. Kim, C. Kang and H. M. Kim, *Chem. Sci.*, 2016, **7**, 3703–3709.
- [9] M. Li, C. Zhai, S. Wang, W. Huang, Y. Liu and Z. Li, *RSC advances.*, 2019, **9**, 40689–40693.
- [10] B. Zhang, S. Qin, N. Wang, X. Lu, J. Jiao, J. Zhang and W. Zhao, *Talanta.*, 2024, **266**, 124971.
- [11] X. Wu, R. Wang, S. Qi, N. Kwon, J. Han, H. Kim, H. Li, F. Yu and J. Yoon, *Angew. Chem.*, 2021, **60**, 15418–15425.
- [12] X. Wu, J. M. An, J. Shang, E. Huh, S. Qi, E. Lee, H. Li, G. Kim, H. Ma and M. S. Oh, *Chem. Sci.*, 2020, **11**, 11285–11292.
- [13] Z. M. Liu, H. J. Du, T. Q. Wang, Y. N. Ma, J. R. Liu, M. C. Yan and H. Y. Wang, *Dyes and Pigments.*, 2019, **171**, 107711.